The relevance of environment vs. composition on dissolved organic matter degradation in freshwaters

Núria Catalán, Ada Pastor, Carles M Borrego, Joan Pere Casas-ruiz, Jeffrey A Hawkes, Carmen Gutiérrez, Daniel Schiller, Rafael Marcé

▶ **To cite this version:**

Núria Catalán, Ada Pastor, Carles M Borrego, Joan Pere Casas-ruiz, Jeffrey A Hawkes, et al.. The relevance of environment vs. composition on dissolved organic matter degradation in freshwaters. Limnology and Oceanography, 2020, 66 (2), pp.306 - 320. ⟨10.1002/lno.11606⟩. ⟨hal-03699378⟩

HAL Id: hal-03699378

https://hal.science/hal-03699378v1

Submitted on 20 Jun 2022

HAL is a multi-disciplinary open access archive for the deposit and dissemination of scientific research documents, whether they are published or not. The documents may come from teaching and research institutions in France or abroad, or from public or private research centers.

L'archive ouverte pluridisciplinaire **HAL**, est destinée au dépôt et à la diffusion de documents scientifiques de niveau recherche, publiés ou non, émanant des établissements d'enseignement et de recherche français ou étrangers, des laboratoires publics ou privés.

HAL Authorization

LIMNOLOGY and OCEANOGRAPHY

ASLO

Limnol. Oceanogr. 9999, 2020, 1–15
© 2020 The Authors. *Limnology and Oceanography* published by Wiley Periodicals LLC. on behalf of Association for the Sciences of Limnology and Oceanography.
doi: 10.1002/lno.11606

The relevance of environment vs. composition on dissolved organic matter degradation in freshwaters

Núria Catalán,[1,2,7,8*,†] **Ada Pastor**,[1,3,†] **Carles M. Borrego**,[1,4] **Joan Pere Casas-Ruiz**,[1,9] **Jeffrey A. Hawkes**,[5] **Carmen Gutiérrez**,[1,2] **Daniel von Schiller**,[6] **Rafael Marcé**[1,2]

[1]Catalan Institute for Water Research (ICRA), Girona, Spain
[2]Universitat de Girona, Girona, Spain
[3]Department of Bioscience, Aarhus University, Aarhus, Denmark
[4]Group of Molecular Microbial Ecology, Institute of Aquatic Ecology, University of Girona, Girona, Spain
[5]Department of Chemistry, BMC, Uppsala University, Uppsala, Sweden
[6]Department of Evolutionary Biology, Ecology and Environmental Sciences, University of Barcelona, Barcelona, Spain
[7]Present address: United States Geological Survey, Boulder, Colorado
[8]Present address: Laboratoire des Sciences du Climat et de l'Environnement, LSCE, CEA, CNRS, UVSQ, Gif-Sur-Yvette, France
[9]Present address: Research Group on Ecology of Inland Waters (GRECO), Institute of Aquatic Ecology, University of Girona, Girona, Spain

Abstract

Dissolved organic matter (DOM) composition exerts a direct control on its degradation and subsequent persistence in aquatic ecosystems. Yet, under certain conditions, the degradation patterns of DOM cannot be solely explained by its composition, highlighting the relevance of environmental conditions for DOM degradation. Here, we experimentally assessed the relative influence of composition vs. environment on DOM degradation by performing degradation bioassays using three contrasting DOM sources inoculated with a standardized bacterial inoculum under five distinct environments. The DOM degradation kinetics modeled using reactivity continuum models showed that composition was more important than environment in determining the bulk DOM decay patterns. Changes in DOM composition resulted from the interaction between DOM source and environment. The role of environment was stronger on shaping the bacterial community composition, but the intrinsic nature of the DOM source exerted stronger control on the DOM degradation function.

A great proportion of the net production of terrestrial ecosystems reaches freshwaters, where organic carbon is accumulated, processed, or transported to oceans (Cole et al. 2007). Excluding lake sediments, the largest reservoir of carbon in freshwater ecosystems is also the most dynamic: dissolved organic matter (DOM). DOM is a complex amalgam of organic compounds of both terrestrial and aquatic origin and is a central component of the biogeochemistry and ecology of freshwater ecosystems (Prairie 2008). The chemical complexity inherent to DOM exerts a direct control on its degradation and subsequent persistence in aquatic ecosystems (Dittmar 2014; Kellerman et al. 2015). The reactivity of DOM is thus often perceived as an intrinsic property of DOM that relies exclusively on its chemical complexity. However, growing evidence from soil studies indicates that the persistence of organic matter is controlled by the interaction of its chemical properties with the physicochemistry and biology of the environment (Schmidt et al. 2011; *see* Kleber 2010 for a critical review). Accordingly, the degradation and persistence of soil organic matter is primarily not a molecular property, but an ecosystem one. Similar concepts have developed in marine biogeochemistry, where ecosystem properties constrain the rate of organic matter degradation (Dittmar 2014). Recently, mineral protection has been described as a central control on

*Correspondence: ncatalangarcia@gmail.com

This is an open access article under the terms of the Creative Commons Attribution License, which permits use, distribution and reproduction in any medium, provided the original work is properly cited.

Additional Supporting Information may be found in the online version of this article.

Author Contribution Statement: According to CRediT categories, authors contributed to conceptualization and experimental design (A.P., N.C., C.M.B., C.G., D.v.S., J.P.C.-R., R.M.); data curation (A.P., N.C., C.M.B., J.P.C.-R.); formal analysis (A.P., N.C., C.M.B., J.P.C.-R., J.A.H.); funding acquisition (R.M.); experimental setup (A.P., N.C., C.G., D.v.S., R.M.); experimental analysis (A.P., N.C., C.G., C.B., J.P.C.-R., J.A.H.); project administration (C.G., R.M.); resources (C.G., C.M.B., R.M.); supervision (R.M.); validation (A.P., N.C., C.G., C.M.B., R.M.); visualization (A.P., N.C., J.A.H.); initial draft (N.C.); and review and editing (A.P., N.C., C.M.B., C.G., D.v.S., J.A.H., J.P.C.-R., R.M.).

[†]Equally contributing authors.

organic carbon preservation across systems (Hemingway et al. 2019) and numerous examples show compounds often considered "recalcitrant," such as organic matter with ancient radiocarbon age, rapidly turning over under certain conditions, such as when physical barriers disappear (Schmidt et al. 2011; McCallister and Del Giorgio 2012). An extreme example for such a situation is following permafrost thawing, where old carbon that resisted degradation for millennia can be easily mineralized (Mann et al. 2015). This view is also starting to be incorporated in freshwater science (Marín-Spiotta et al. 2014; but *see* Sinsabaugh and Findlay 2003 for an early example), implying that the location of the DOM reaction (e.g., sediments, water column, hyporheic zone) will determine the physical framework, and consequently, the intensity of DOM degradation. Nevertheless, most evidence available from freshwaters points toward a preferential loss of organic compounds based on their composition (Kellerman et al. 2015) linked to the effect of the microbial community (D'Andrilli et al. 2019).

The link between molecular composition and microbial community is conceptually and methodologically at the core of the study of DOM reactivity in freshwaters, while ecosystem properties are often overlooked (Sinsabaugh and Findlay 2003). The growing availability and understanding of high-resolution mass-spectrometry (Koch et al. 2008; Patriarca et al. 2018) has allowed the identification and alignment of the formulae of thousands of compounds across DOM samples (Kujawinski et al. 2002). The degradation of these compounds is expected to be driven by specific relationships between the individual compounds and the metabolic potential of the resident microbiota (Moran et al. 2016). However, multiple constraints remain on identifying biogeochemically relevant genes for DOM degradation (Logue et al. 2016; Osterholz et al. 2016), and thus, on establishing such relationships. This is partly a consequence of the functional redundancy concomitant to the DOM biodegradation function (Roger et al. 2016) and the lack of knowledge on the intermediate metabolites of different degradation pathways, that could account for a large part of DOM chemical diversity (Wienhausen et al. 2017). Additionally, and despite the usefulness of high-resolution methods, technical limitations lead to the risk of asking "method-driven questions" (Lakhotia 2009). The wealth of data generated can lead to the determination of false positive trends, particularly under the assumption that DOM molecular-level properties are at the center of functional responses and drive DOM degradation processes without clear prior evidence. Most analytical techniques for DOM characterization have restrictive "analytical windows" (e.g., fluorescence requires a fluorophore, electrospray ionization requires polarity, solid phase extraction requires hydrophobicity), so results are highly biased toward certain groups of compounds. These limitations need to be discussed when interpreting DOM compositional changes during incubations.

Here, we aimed at experimentally disentangling the relative role of environment and composition on DOM degradation in freshwaters. We borrow a simile from cancer research (Mukherjee 2017) by asking what is more important in controlling DOM decay rates: the *soil* (i.e., environmental conditions) or the *seed* (i.e., composition of DOM)? To test this, we conducted a controlled degradation experiment on three contrasting DOM sources under five environments that were selected to cover a wide spectrum of environmental conditions frequently found in freshwaters. To understand the relevance of environmental vs. compositional factors, it is crucial to rule out the "microbial factor," that is, the effect of using disparate microbial communities on DOM degradation experiments. Thus, we used a standard bacterial inoculum composed of six culturable strains that were previously tested to be functionally and metabolically versatile (Pastor et al. 2018) (Fig. 1a). The use of the standard bacterial inoculum allows for a standardization of the effects of different metabolic capacities on the degradation rates and concomitant DOM compositional changes. To assess DOM degradation dynamics, we tracked the changes through time in DOM amount and composition across sources and environments. In addition, we assessed the effect on the composition of the standard bacterial inoculum. Based on the across-ecosystems emerging view, we hypothesize that the environment exerts a stronger control than DOM composition on the degradation kinetics of DOM in freshwaters. Accordingly, we expected a consistent effect of a given environment on DOM composition and postulate that it is the environment and not the DOM source that drives the variability in DOM degradation kinetics (Fig. 1b), linked to a stronger effect of the environment than of the DOM source on the microbial community.

Material and methods

Collection and preparation of DOM sources

We selected three DOM sources commonly present in aquatic ecosystems which are known to vary in their DOM properties and consequently functional role (i.e., composition, bioavailability, and susceptibility to UV light among others). DOM amendments were thus prepared from algae cultures (DOM_{Algae}), alder leaf leachates (DOM_{Leaf}), and Suwannee River natural organic matter (DOM_{Humic}). We extracted DOM_{Algae} from a common green algae culture (*Scenedesmus obliquus*). The culture was sonicated (10 min), frozen overnight, thawed, and sonicated again (10 min) in a precombusted glass bottle. The solution was prefiltered onto precombusted GF/F filters (Millipore) and subsequently filtered through 0.1 μm filters (Durapore®, Millipore). The resulting leachate was stored refrigerated at 4°C prior to the start of the experiment, which was conducted within the next 2 d. For DOM_{Leaf}, leachates were derived from freshly fallen alder leaves (*Alnus glutinosa*; a common riparian tree in Europe) harvested in autumn, rinsed with distilled water, and air-dried to constant weight. Prior to leaching, plant material was cut into < 2.5 cm pieces and homogenized. Leaching was conducted in Milli-Q water for 4 d (150 rpm; 4°C) in complete darkness using precombusted glass bottles. Even at 4°C, microbial growth

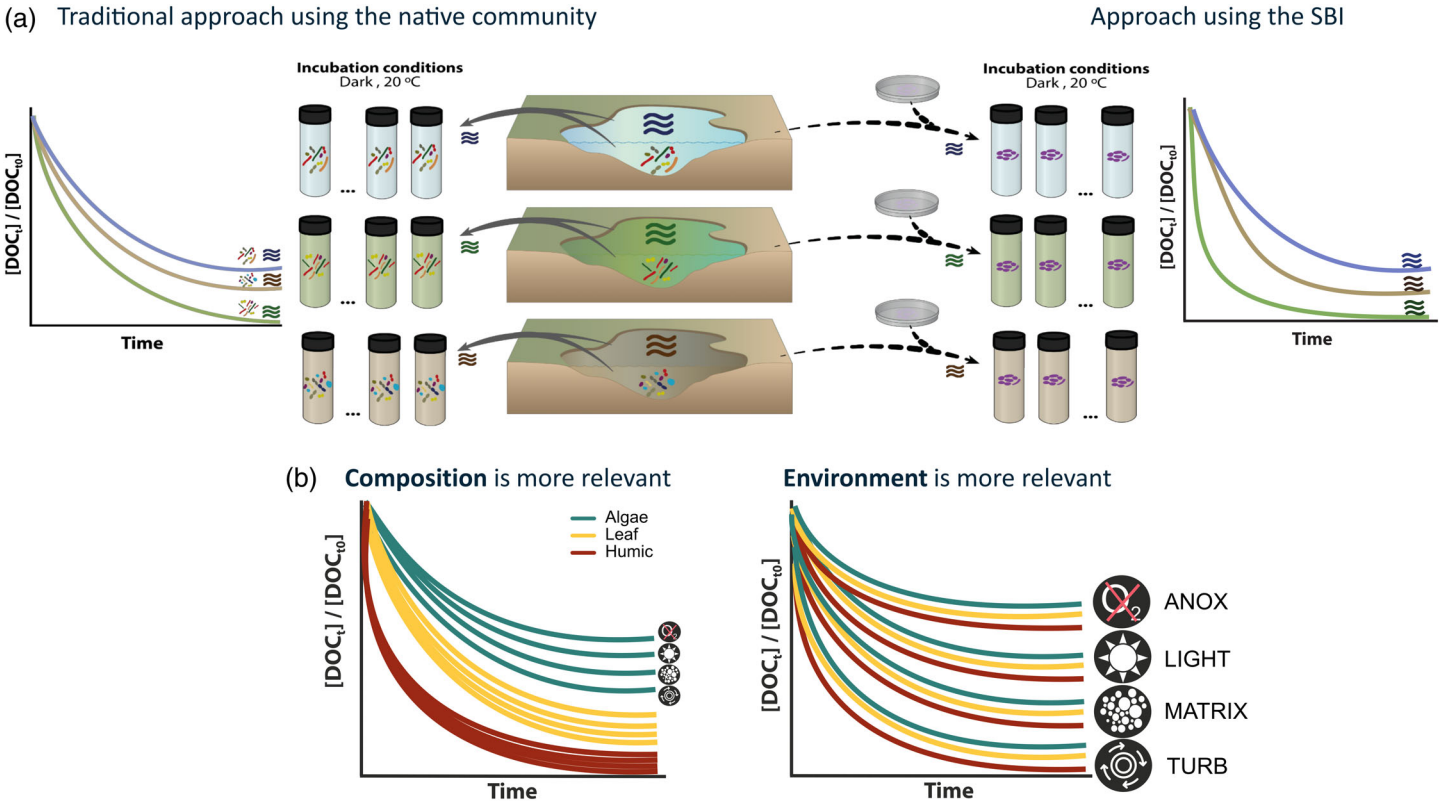

Fig 1. Conceptual approach and hypothesis. (**a**) Traditional approach using the native microbial community of each site vs. the approach using the standard bacterial inoculum (SBI), where the native community is replaced by a common inoculum developed in lab cultures as described in Pastor et al. (2018). The use of the SBI allows to rule out the effect of using disparate microbial communities on DOM degradation experiments of different DOM sources. (**b**) Experimental design and hypothesis, if composition of contrasting DOM sources is more relevant (left panel), degradation kinetics of a given source should be more similar between them than if the environment is more relevant (right panel). Here, the DOM sources selected were algae cultures (Algae), alder leaves leachates (Leaf), and Suwannee River Natural Organic Matter (Humic) and are represented in three different colors, the different environments by the symbols beside the lines.

cannot be completely discarded, and some labile compounds might have been consumed during leaching. The supernatant was sieved, prefiltered through precombusted GF/F filters (Millipore), and finally through 0.1 μm filters (Durapore®, Millipore). For DOM_{Humic}, we used Suwannee River natural organic matter concentrate (Ref. 2R101N), provided by the International Humic Substance Society, which is commonly used as a reference sample for humic acids derived from swamp areas (Green et al. 2015).

Environments selected

The definition of the environments was the result of a collective ideation workshop held the 8th October 2015 at the Catalan Institute of Water Research (ICRA) among researchers with different backgrounds (i.e., chemistry, microbiology, and biogeochemistry), and based on strategic design techniques tools (i.e., research map and semantic profile techniques; Argote and Levine 2020). These techniques were used to generate target-discussions and to collectively pinpoint the relevant aquatic environments for DOM degradation that were feasible to reproduce in laboratory conditions (*see* Section 2 in Supporting Information for details). Because the objective of this study was not to understand the effect of the single environmental gradients, but to test the effects on DOM degradation of environments in relation to DOM properties, we selected this approach where "Environment" is considered as a factor with five levels (Fig. 1b). As a result, we selected five contrasting artificial environments to be tested, including the presence of turbulence ($Environment_{Turbulence}$), the presence of a physical matrix offering contact surface ($Environment_{Matrix}$), the presence of UV-light ($Environment_{UVLight}$), and the absence of oxygen ($Environment_{Anoxic}$), in addition to a control ($Environment_{Control}$).

Experimental setup

Treatments with the different DOM sources were prepared with organic carbon-free artificial lake water (Supporting Information Table S6.1) in 7-liter acid-washed plastic containers. The initial concentration was ≈ 5 mg C L^{-1} based on mean dissolved organic carbon (DOC) values for a range of natural waters (Sobek et al. 2007). For the anoxic environment, the solution was bubbled overnight with N_2 gas to remove O_2.

Containers were amended with the standard bacterial inoculum suitable for DOM degradation bioassays, to an estimated final bacterial density of $\approx 5 \times 10^6$ CFU mL^{-1}. The standard bacterial inoculum is composed of six bacterial strains known to be versatile in the use of organic compounds (*Arthrobacter phenanthrenivorans*, *Bacillus licheniformis*, *Exiguobacterium sibiricum*, *Paracoccus denitrificans*, *Burkholderia multivorans*, and *Pseudomonas putida*; Pastor et al. 2018). Each solution was distributed into acid-washed, precombusted (450°C for 4 h) 40-mL glass vials, which were sealed headspace free with Teflon-coated septa. For Environment$_{\text{Anoxic}}$, the standard bacterial inoculum was introduced into the experimental vials in an anaerobic chamber (Coy Lab Products, Michigan, U.S.A.). All vials were incubated at 20°C, in the darkness (except those in the Environment$_{\text{UVLight}}$) and randomly distributed among the five environments.

In the case of the Environment$_{\text{Control}}$, no further treatment was applied to those vials during incubation (Fig. 1). The Environment$_{\text{Turbulence}}$ was created by agitating the vials with a plate shaker (150 rpm). Surface availability in the Environment$_{\text{Matrix}}$ was increased by adding 2 g of acid-washed precombusted glass beads (425–600 μm; Sigma, U.S.A.) to the vials. In the Environment$_{\text{UVLight}}$, vials were horizontally exposed to artificial light (Philips Actinic BL 36W) with emission maximum in the UV-A band (average measured values 21.2 W m^{-2}) during the whole incubation period.

Each combination of factors levels (DOM$_{\text{source}}$ × Environment) was fourfold replicated and sampled for DOC concentration at the initial time and at days 1, 3, 7, 14, 21, and 28 after the start of the incubation. Moreover, we collected samples for optical characterization (four replicates) and DNA analyses (three replicates) at the initial and final time. Different subsets of vials were prepared and sacrificed at each experimental time. All the incubations started with the same bacterial abundance (1.6×10^6 cells mL^{-1}). The treatment DOM$_{\text{Algae}}$ × Environment$_{\text{UVLight}}$ was excluded from further consideration, as algal growth was detected.

DOC concentration, DOM optical spectroscopy, and parallel factor analysis

Samples from the incubations for DOC concentration were acidified with 10% HCl to a pH between 2 and 3 and analyzed by high-temperature catalytic oxidation on a Shimadzu TOC-V CSH analyzer (Shimadzu Corporation, Japan). The biodegradable fraction of DOC (%) was assessed by determining change in DOC concentration between the end of incubation (28 d) and the average initial concentration among replicates. The total biodegradable DOC proportion ranged from 7% (DOM$_{\text{Algae}}$ × Environment$_{\text{Matrix}}$) to 57% (DOM$_{\text{Leaf}}$ × Environment$_{\text{UVLight}}$).

Excitation-emission matrices were obtained on samples at room temperature using a F-7000 (Hitachi, Japan) spectrofluorometer with a 1-cm quartz cuvette. Excitation-emission matrices were acquired across the excitation range from 248 to 449 nm (3 nm increments) and the emission range from 250 to 550 nm (3 nm increments). Excitation and emission slit widths were set to 5 nm. Sample to reference signal ratio mode and instrument-specific biases correction were used on all Excitation-Emission matrices, and a Milli-Q water blank collected every 10 samples was subtracted from the Excitation-Emission matrices. Spectra were corrected for inner filter effects according to criteria in Kothawala et al. (2013) and using UV–Visible absorbance spectra (190–800 nm) measured on an Agilent 8453 diode array spectrophotometer (Agilent Technologies, Germany). The integral of the Raman scatter peak of Milli-Q blanks was used for Excitation-Emission matrices intensity calibration to Raman Units (Murphy et al. 2010). These corrections were implemented using an internal laboratory routine running in MATLAB (MathWorks, Inc.).

Parallel factor analysis (PARAFAC) was used over 122 samples to identify the main components of the Excitation-Emission matrices according to Murphy et al. (2013). Rayleigh scatter was replaced by a band of missing data, and each sample was normalized to its total fluorescence prior to fitting the PARAFAC model. Potential model outliers were evaluated by examining residuals and leverage of each sample. The appropriate number of components was determined by visual inspection of the residual fluorescence and the spectral shape of the components according to organic fluorophores. The model was then validated by split-half analysis and random initialization with 15 iterations. Four PARAFAC components (C1, C2, C3, and C4; Fig. 3) were validated. Components C2, C3, and C4 corresponded to humic-like materials and C1 to protein-like fluorescence. The results of the PARAFAC model were queried (Tucker's congruence coefficient = 95%) in order to search for quantitative matches with previously validated PARAFAC using the OpenFluor database (https://openfluor.lablicate.com/; accessed June 2019) (Murphy et al. 2014). Details on the matches with previous models are provided in Section S5 in Supporting Information. Briefly, component C1 exhibits a protein-like signal that has been linked to recent biological activity and found across seawater, freshwater, and artificial systems. Humic-like component C2 resembles fluorescence peaks A and C. C3 was particularly prominent in our DOM$_{\text{Leaf}}$ and is related with sources from terrestrial soils. C4 is related to peak M (processed humic materials and microbial activity). The relative change in the components was calculated as: $(\text{Int } C_{\text{iFinal}} - \text{Int } C_{\text{iInitial}})/\sum(\text{Int } C_{\text{i}\rightarrow\text{j Initial}}) \times 100)$, where Int C_i is the intensity of a given component at Initial or Final incubation time.

Reversed-phase high-performance liquid chromatography coupled to electrospray ionization high-resolution mass spectroscopy (HPLC-ESI-HRMS)

Samples from the incubations were acidified using reagent grade HCl (Merck) 1 mol L^{-1} to pH 2–3 and loaded onto prewashed and conditioned solid-phase extraction cartridges (Agilent PPL, 100 mg), according to Dittmar et al. (2008).

All the available volume (i.e., 40 mL) was loaded in all samples, which, because samples were expected to have around 5 mg L^{-1}, meant that we expected 200 μg C to be loaded. The cartridges were washed with 3 mL of 0.1% HCl acid and the solid-phase-extracted DOM was eluted with 2 mL methanol.

Extracted methanol for ultrapure water blank and the three $DOM_{sources}$ was dried in a vacuum centrifuge (Eppendorf Concentrator Plus). Five hundred microliters was dried for the blank, Algae, and Leaf samples and 250 μL was dried for the Humic sample due to higher abundance of carbon. The dried samples were redissolved in 50 μL mobile phase A (*see* below). Thirty-microliter sample was injected onto the high-performance liquid chromatography (HPLC) column (Kinetex polar-C18 column 100 × 2.1 mm, 2.6 μm; Phenomenex). The chromatographic separation was conducted with an Agilent 1100 HPLC system with flow rate set to 220 μL min^{-1} using two mobile phases, A: 0.1% formic acid in ultrapure water, and B: 80% acetonitrile, 0.1% formic acid in ultrapure water. Sample was loaded with 1% B, which was maintained for 1.5 min, before ramping to 99% B over 18.5 min. 99% B was held until 23 min, then the phase was returned to 1% B by 24 min and held isocratic until 30 min to re-equilibrate the column. The retained material was detected by negative mode ESI-HRMS (Orbitrap Velos Pro, Thermo Fisher, Germany).

Electrospray ionizable material was assigned to formulas and its intensity across the separation summed. Formula assignment used a theoretical framework of possibilities as follows: C 4:40, H 4:80, O 0:35, N 0:1, S 0:1, 13C 0:1, m/z 120–700, mass error < 3 ppm, mass defect −0.1 to 0.3, H/C 0.3–2, O/C ≤ 1, double bond equivalence minus oxygen ≤ 10. Detected peaks were considered as those greater than the mean + 3 × standard deviation (SD) of noise in the transient, where noise was determined as intensity with mass defect 0.6–0.8. The resulting assignments were summed across the chromatographic separation and filtered to remove molecular assignments that were less than 3× the blank sample.

DNA extraction, amplicon-targeted sequencing, and processing

The molecular analyses described here were carried out to monitor the standard bacterial inoculum strains during incubation time and to identify any potential external microbial contamination. Three vials (42 mL) incubated in the same conditions were extracted for DNA using a combination of enzymatic cell lysis with lysozyme and proteinase K followed by a modified CTAB extraction protocol as previously described (Llirós et al. 2008). Concentration of DNA in each extract was determined fluorometrically using a QUBIT®2.0 Fluorometer (Invitrogen Molecular probes, Inc., Oslo, Norway).

For community analysis, DNA extracts were sequenced, merged, filtered, chimera checked, and clustered into operational taxonomic units (OTUs) as described in Subirats et al. (2019); *see* Section S4 in Supporting Information). Sequencing depth ranged between 4819 and 71,330 sequences per sample. The sample with the lowest sequence number (NCFE03, 4810 sequences) was removed from downstream analysis. OTUs affiliated to Archaea (2; 0.4%) and unclassified (4; 1.4%) were filtered from the original OTU table using QIIME (Caporaso et al. 2010). After filtering, we obtained a total of 277 bacterial OTUs. Considering that the initial inoculum only contained six species (Pastor et al. 2018), the final number of OTUs delineated from the sequence dataset likely resulted from spurious OTUs generated during the sequencing process. Indeed, most OTUs were unevenly distributed across treatments and showed relative abundances < 1% across samples, thus suggesting that they were either sequencing artifacts or remnants of microorganisms present in DOM sources (algal or leaf biomass). The OTU table was then filtered to remove spurious OTUs (occurring at a relative abundance < 1% across samples) using appropriate scripts in QIIME. After filtering, we only retained 12 OTUs, six of them (OTU-1 to -6) affiliated to the six species in the standard bacterial inoculum. For community analysis, the number of sequences in each sample was normalized by randomly selecting a subset of 30,000 sequences per sample to minimize bias due to different sequencing depth across samples. Besides, the number of sequences of each OTU was further corrected for the average number of rRNA operons in the genomes of standard bacterial inoculum members. The average values used for this calculation were obtained from the Ribosomal RNA Database (http://rrndb.umms.med.umich.edu/; accessed in June 2018; Lee et al. 2009).

Data treatment

DOC degradation kinetics were modeled using a reactivity continuum model, with a Gamma distribution as the initial distribution of reactivities, according to Koehler et al. (2012). Model parameters were estimated using nonlinear regression package *nlme* in R (Pinheiro et al. 2018). In the full model, a factor generated as the interaction of the two study factors (DOM_{source} and Environment) was used to fit a nonlinear mixed-effects model over a list of nonlinear least squares models using the function *nlme.nlsList*, thus obtaining a reactivity continuum model for each combination of factor levels (m0; models parameters in Table 1). In order to test for the effect of the two factors, and to avoid running out of degrees of freedom, we built three models (results in Table 2): Model 1 with DOM_{source} as fixed effect; Model 2 with Environment as fixed effect, and Model 3 both factors (DOM_{source} + Environment). Significance of the fixed effect was evaluated using ANOVA (*anova.lme* function). Each of these models was tested against m0 and between them. The likelihood ratio comparing the likelihood of Model 1 vs. Model 3 and Model 2 vs. Model 3 was used to compare the effect of the additional factor over the model.

We evaluated the effect of the studied factors (DOM_{source} and Environment) on the relative change of fluorescence

Table 1. Degradation dynamics of the different sources of DOM under the five selected environments. Output of the reactivity continuum models obtained from the full model applied to the DOC degradation. α (apparent age of the most reactive compounds) and ν (relative abundance most persistent compounds) are the model parameters. k initial (h^{-1}) is the initial apparent decay coefficient at time = 0.

Environment	DOM source	α (h)	ν	k initial (h^{-1})	BDOC (%)
Control	Algae	73.1 ± 2.6	0.072 ± 0.008	0.001 ± 0.0006	16.6 ± 1.5
Control	Leaf	17.9 ± 1.4	0.202 ± 0.046	0.0113 ± 0.0039	52.1 ± 2.6
Control	Humic	61.8 ± 2.1	0.088 ± 0.011	0.0014 ± 0.0007	16.9 ± 1.3
Turbulence	Algae	5.9 ± 2.7	0.043 ± 0.002	0.0073 ± 0.0094	15.3 ± 1.8
Turbulence	Leaf	17.8 ± 1.4	0.197 ± 0.044	0.0111 ± 0.0042	52.9 ± 2
Turbulence	Humic	26.4 ± 3.1	0.045 ± 0.003	0.0017 ± 0.0009	14.4 ± 0.5
UV-light	Algae	Increase	Increase	Increase	Increase
UV-light	Leaf	47.9 ± 1.3	0.314 ± 0.111	0.0066 ± 0.0024	56.6 ± 1.2
UV-light	Humic	122.2 ± 1.6	0.231 ± 0.068	0.0019 ± 0.0007	34.2 ± 1.5
Matrix	Algae	183.9 ± 16.9	0.045 ± 0.01	0.0002 ± 0.0002	7.4 ± 1.5
Matrix	Leaf	14.6 ± 1.5	0.136 ± 0.021	0.0094 ± 0.0042	45.2 ± 1.9
Matrix	Humic	107.6 ± 3.9	0.062 ± 0.008	0.0006 ± 0.0006	14.1 ± 4.4
Anoxic	Algae	13.4 ± 2.2	0.063 ± 0.005	0.0047 ± 0.0033	21.2 ± 1.1
Anoxic	Leaf	31.3 ± 1.4	0.210 ± 0.05	0.0067 ± 0.003	50.6 ± 3.2
Anoxic	Humic	83.2 ± 3.6	0.076 ± 0.01	0.0009 ± 0.0012	10.7 ± 1.9

Values for the model parameters are predicted estimates and associated standard errors (SEs). SE for k corresponds to the combined errors of α and ν. BDOC corresponds to mean values and SDs (n = 4).
DOM sources correspond to algae cultures (Algae), alder leaves leachates (Leaf) and Suwannee River Natural Organic Matter (Humic) and Environments to Control, Turbulence, UV-light Matrix, and Anoxic.
BDOC, biodegradable dissolved organic carbon.

Table 2. ANOVA tests to compare the likelihood of the fixed effects models. To test for the effect of the two factors, and to avoid running out of degrees of freedom, we built three models: Model 1, DOM_{source} as fixed effect; Model 2, environment as fixed effect; and Model 3, DOM_{source} + environment. Significance of the fixed effect was evaluated using ANOVA (*anova.lme* function in R). The results of the likelihood ratio test comparing Model 1 and Model 2 with model 3 are shown here.

ANOVA (Model 2, Model 3)

Model	df	log Lik	Test	Log likelihood ratio	p value
Model 2 (Environment)	14	617.1393	1 vs. 2	36.16271	$p < 0.0001$
Model 3 (DOM_{source} + Environment)	18	635.2207			
ANOVA (Model 1, Model 3)					
Model	**df**	**log Lik**	**Test**	**Log likelihood ratio**	**p value**
Model 1 (DOM_{source})	10	623.6755	1 vs. 2	23.0903	$p = 0.0033$
Model 3 (DOM_{source} + Environment)	18	635.2207			

components during the incubations with type II ANOVA including the interaction term, using the *Anova* function in *car* package (Fox and Weisberg 2011). Statistical analyses were performed in R 3.5.3 (R Core Development Team, 2016).

For microbial community composition, abundance boxplots were built in R 3.1.1 using package *ampvis2* (Andersen et al. 2018) after loading the filtered OTU table generated in QIIME. The same OTU table was uploaded into *phyloseq* (McMurdie and Holmes 2013) in R to run a Detrended Canonical Analysis using the Bray Curtis distance matrix on Hellinger-transformed abundance data. Prior to analysis, relative abundances of OTUs were corrected according to the rRNA operon copy number of their taxonomic group and filtered by abundance (1% cutoff, see above).

Results

Factors controlling DOM decay patterns

Reactivity continuum models described well the degradation of DOC in all treatments (Table 1; Fig. 2). We observed a marked decay of the DOM_{Leaf} across Environment levels, while the kinetics were more similar for the DOM_{Algae} and DOM_{Humic}. The mean average lifetime of the most reactive compounds (α) was highest for the DOM_{Humic}, with the

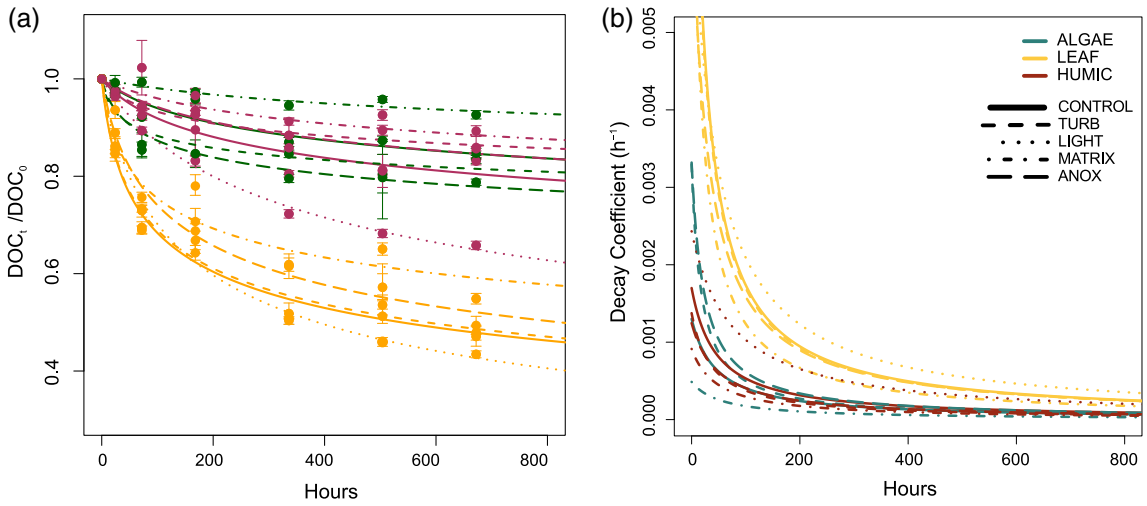

Fig 2. Output of the reactivity continuum model on bulk DOC. (**a**) Mean (± SE) relative decrease in DOC concentration over time during the incubations. The lines show the relative DOC predicted by the reactivity continuum model. (b) Density functions of the models, showing the apparent decay coefficient (*k*) over incubation time for the different DOM sources (colors: algae cultures [algae], alder leaves leachates [leaf], and Suwannee River Natural Organic Matter [humic]) and environments (line types: control, turbulence, UV-light, matrix, and anoxia).

longest lifetime in the Environment$_{UVLight}$, and shortest for the DOM$_{Leaf}$ across environments. The parameter ν, related to the shape of the distribution at $k = 0$, (i.e., lower values, higher relative preponderance of degradation-resistant compounds), was the highest for DOM$_{Leaf}$ and lowest for the DOM$_{Algae}$. This resulted in predicted k declining less pronouncedly in the DOM$_{Leaf}$ (across environments) and the DOM$_{Humic}$ × Environment$_{UVLight}$ treatment (Fig. 2b). The probability distributions of initial reactivity (Supporting Information Fig. S3.1) showed that around 20% of the DOC in the DOM$_{Leaf}$ as well as in the DOM$_{Algae}$ was decaying at fast rates ($k > 0.01$ h^{-1}). In contrast, in the Environment$_{Matrix}$ for both DOM$_{Algae}$ and DOM$_{Humic}$, that fraction represented only around 1% of DOC, with almost 90% decaying at low rates ($k < 0.001$ h^{-1}).

To assess the effects of Environment vs. DOM$_{source}$ on the degradation kinetics of DOM, we evaluated the log-likelihood of two reactivity continuum mixed effects models that have either Environment or DOM$_{source}$ as fixed factors, and a full model that had both (*see* "Material and methods" section). The results of the individual mixed effect models indicated that both Environment and DOM$_{source}$ had a significant effect on the reactivity continuum model parameters, thus on determining the bulk DOM decay (Tables **1** and 2). However, when we tested a model having both factors (Environment + DOM$_{source}$) against the individual models, the respective likelihood ratios indicate that adding DOM$_{source}$ to the Environment model had greater effect (Likelihood ratio statistic: 36.16; $p < 0.0001$) than adding Environment to the DOM$_{source}$ model (Likelihood ratio statistic: 23.09; $p = 0.0033$). Therefore, the DOM source has a stronger impact on defining DOM degradation kinetics than the environment where such degradation occurs.

DOM composition of the three sources and changes during incubation

The DOM sources showed contrasting molecular features and fluorescence signals (Supporting Information Figs. S1.1, S1.2). The solid phase extraction efficiency was very contrasted between DOM sources with mean values of 18% ± 20% for algae, 38% ± 15% for leaf extracts, and 47% ± 17% for humic. The extracted material was clearly different when measured by HPLC-ESI-HRMS. The DOM$_{Algae}$ sample had the lowest HPLC-ESI-HRMS response, as expected due to the low abundance of extractable material. The assigned material was hydrophobic and relatively saturated (H/C > 1.0) compared with a large portion of material in the DOM$_{Humic}$. DOM$_{Humic}$ had a very broad chromatographic distribution, as is typical for aquatic DOM (Hawkes et al. 2018; Patriarca et al. 2018). DOM$_{Leaf}$ was also broadly retained, but with much less hydrophilic material (retention time < 6 min, O/C > 0.6) compared with the DOM$_{Humic}$. The chromatogram for leaf material was also considerably more feature rich compared with the smooth profile of DOM$_{Humic}$, indicating slightly less isomeric diversity and a less degraded state. The three DOM$_{sources}$ were thus highly different in character (percent and character of extractable material). Because the extraction efficiency was so poor for the algae sample, we did not pursue solid phase extraction followed by HPLC-ESI-HRMS as a characterization tool for this study, as only two of the DOM sources could be reasonably well characterized this way.

The DOM$_{Humic}$ fluoresced mainly in the humic-like region of peaks A and C. The DOM$_{Leaf}$ showed maxima at shorter wavelengths corresponding to the humic-like region of peaks A/M and a secondary maximum in the protein-like region.

Finally, the DOM_{Algae} showed lower fluorescence, with signal across the different regions and a relatively weak maximum in the protein-like region. The PARAFAC model revealed four independent components (C1–C4; Fig. 3; Section S5 in Supporting Information). Component C1 corresponds to protein-like fluorescence, components C2 and C3 to humic-like fluorophores, and C4 to a humic-like, microbially derived fluorophore (*see* "Material and methods" section). The relative changes in the PARAFAC fluorescence components at the end of the incubation were tested for each treatment to assess whether the change in each component was linked to Environment or initial DOM_{source} (Fig. 3). Overall, while a component for a given DOM_{source} tended to behave the same across environments, a given environment did not have the same effect across $DOM_{sources}$. Protein-like component C1 decreased across all treatments (Fig. 3a), with Environment and DOM_{source} having a statistically significant effect on its relative intensity change. This effect was higher for DOM_{source} and their interaction was not statistically significant (DOM_{source}: $F_{2,45} = 44.43$; $p < 0.001$; Environment: $F_{4,45} = 13.37$, $p < 0.001$). In the case of the humic-like components C2 and C3, both factors and their interaction were statistically significant (DOM_{source}: $F_{2,44} = 3.72$, $p < 0.05$; Environment: $F_{4,44} = 50.55$, $p < 0.001$; $DOM_{source} \times$ Environment: $F_{8,44} = 56.04$, $p < 0.001$). But, in the case of C2, this interaction had a stronger influence, most likely linked to the effect of the $Environment_{UVLight}$ over DOM_{Humic} (Fig. 3b). In the case of C3, on the contrary, DOM_{source} exerted the strongest influence, with a very marked behavior of this component for DOM_{Leaf} across environments (Fig. 3c; DOM_{source}: $F_{2,45} = 54.6$, $p < 0.001$; Environment: $F_{4,45} = 3.36$, $p < 0.05$; $DOM_{source} \times$ Environment: $F_{8,44} = 8.7$, $p < 0.001$). C4 was the only fluorescence component affected by Environment but not DOM_{source}, although the interaction between DOM_{source} and Environment was significant and in most cases the changes in C4 did not statistically differ from zero (Fig. 3d; Environment: $F_{4,42} = 50.55$, $p < 0.001$; $DOM_{source} \times$ Environment: $F_{8,42} = 2.93$, $p = 0.01$).

Composition of bacterial communities

After quality and abundance data-filtering (*see* "Material and methods" section), we retained 12 OTUs, six of which affiliated to bacterial genera corresponding to the six strains in the standard bacterial inoculum (*Paracoccus* [OTU-1], *Exiguobacterium* [OTU-2], *Pseudomonas* [OTU-3], *Burkholderia* [OTU-4], *Arthrobacter* [OTU-5], and *Bacillus* [OTU-6]). The cumulative relative abundance of these six OTUs at initial time ranged from 99.3% to 100% across all treatments,

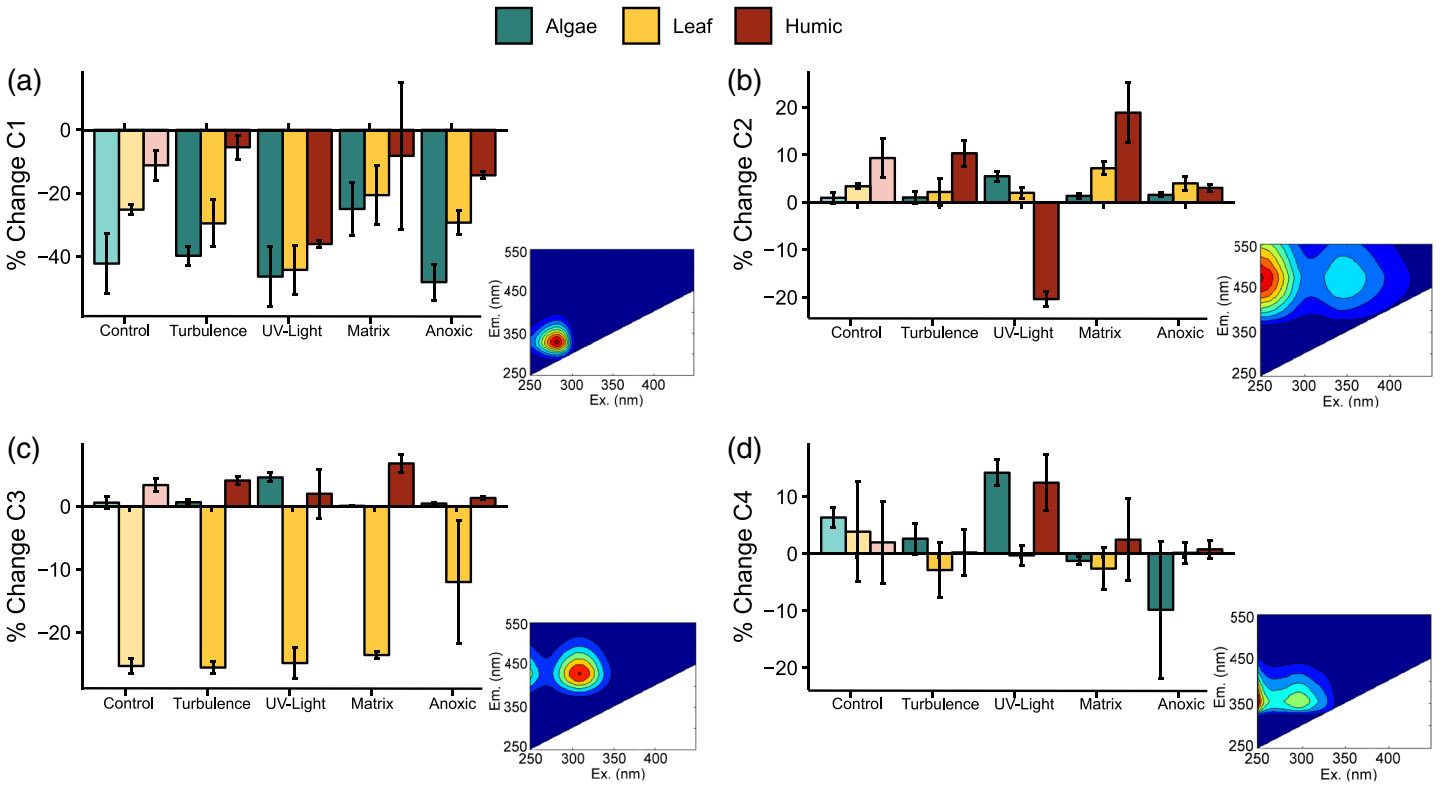

Fig 3. Relative intensity change of the PARAFAC components (**a**) C1, (**b**) C2, (**c**) C3, and (**d**) C4 during the incubations. The shape of each component within the excitation-emission matrix is shown in the insets. DOM sources correspond to algae cultures (Algae), alder leaves leachates (Leaf), and Suwannee River Natural Organic Matter (Humic) and environments to control, turbulence, UV-light, matrix, and anoxic.

validating the homogenous composition of the bacterial community at initial conditions. After incubation, the average relative contribution of the six standard bacterial inoculum strains across treatments was 78.1% ± 19.1%, ranging from 41.2% ± 4.21% (Light environment) to 90.2% ± 7.25% (Control) (Fig. 4).

To assess how bacterial communities responded to factors (DOM_{source} and Environment), we ran an analysis of beta-diversity according to the Bray-Curtis similarity distance. Ordination of samples using a Detrended Canonical Analysis explained 63.9% of the variance in community composition (Fig. 5) and indicated that changes in the microbial community throughout the biodegradation experiments were more linked to Environment than to DOM_{source}, although both affected community composition. Particularly, the first Detrended Canonical Analysis axis (39.0% of total variance) clearly separates $Environment_{UVLight}$ and $Environment_{Anoxic}$ from one another and from the rest of environments. Despite the conspicuous presence of the six OTUs of the standard bacterial inoculum, samples incubated under light were characterized by an increase in the relative abundance of sequences affiliated to *Sediminibacterium* (OTU-7, average 40.0% ± 13.5%) and *Limnohabitans* (OTU-13, average 16.3% ± 10.1%), whereas under anoxic conditions samples were enriched in sequences affiliated to *Lysobacter* (OTU-10, 16.0% ± 14.3%) (Fig. 4). Samples incubated under $Environment_{Control}$, $Environment_{Turbulence}$, and $Environment_{Matrix}$ clustered together with the initial samples (time 0) along the first axis, indicating that these environments did not induce major changes in the composition of bacterial communities. The second Detrended Canonical Analysis axis (24.9% of the variance) separates initial (with negative values) from final samples but also $DOM_{sources}$. Particularly, samples incubated on DOM_{Leaf} clustered together regardless of environment (Fig. 5). This clustering probably resulted from the specific occurrence in these samples of OTU-8 (*Massilia* spp., average relative abundance of 6.68% ± 3.59%) and OTU-15 (*Pedobacter* spp., 5.90% ± 4.31%) (Fig. 4).

Discussion

Composition prevails over environment in controlling DOM decay, but both are relevant

Bulk DOM decay kinetics were controlled both by the source of DOM and the environment, but the effect of the former was the strongest (Table 2). Therefore, the original composition of DOM had the highest impact on defining its bulk decay, despite the conditions under which this decay took place. This result agrees with previous field studies in freshwaters that observed a strong dependence of the degradation and persistence of DOM on its composition (Creed et al. 2015; Kellerman et al. 2015; Mosher et al. 2015). Mostly, these evidences indicate directional shifts in composition with time in the environment.

The relative lesser importance of the environment was consistent across three DOM sources (leaf litter, algal exudates, and humic organic matter) with very contrasting composition (Section S1 in Supporting Information) and expected functional roles (Sinsabaugh and Findlay 2003). The reactivity continuum models show a very clear distinctive decay of the DOM source from leaf litter (Fig. 2). At a first glance, the decay pattern is not as distinctive for algal exudates and humic DOM as for leaf litter. However, the humic DOM source presents a very robust behavior across environments, with a similar biodegradable DOC fraction and decay rates by the end of the incubation across environments (Table 1; Fig. 2). Even the $Environment_{UVLight}$ on the humic DOM source led to similar decay rates and distribution of the most degradable compounds (Supporting Information Fig. S3.1). The similarity of the decay pattern across treatments suggests that, despite a higher susceptibility to photodegradation, the dominance of unsaturated, aromatic compounds limits humic DOM biodegradation to a similar extent across treatments. In turn, the algal DOM showed a stronger effect of the environment, with contrasting biodegradable DOC fraction values and distribution of probabilities of the compounds across environments (Supporting Information Fig. S3.1). We believe that this contrasted effect of Environments matrix and turbulence or anoxia for algal DOM might be due to (1) its hydrophobicity (Supporting Information Fig. S1.2), which might enhance interaction with matrix, limiting degradation, and (2) its higher bioavailability, so that its degradation is not limited under anoxic conditions. Our selection of DOM sources was meant to represent the wide spectrum of freshwater DOM types and to intensify compositional differences. Therefore, our results reflect the potential role of composition on bulk DOM decay. In situations when similar DOM sources occur in disparate environments, the relative importance of environmental controls is likely to increase or even prevail.

The environments simulated in our experiment cover a wide range of environmental conditions expected to affect DOM persistence in freshwaters, such as contrasting stability, turbulence, light exposure, or oxygen availability (Marín-Spiotta et al. 2014). However, some potentially relevant conditions were not tested in our experiment. For instance, solution chemistry (e.g., ionic strength), which defines the self-assembly of DOM compounds and might promote their aggregation (Chin et al. 1998) and further define their interaction with the solid matrix. Moreover, evidence at the geological time scale points out the relevance of mineral protection on DOM persistence across ecosystems (Hemingway et al. 2019). Such protection results from the interaction between oxidant availability, mineral surface area and charge, and organic matter composition. The latter might be of particular relevance in freshwater ecosystems according to our results. Further investigation using contrasting solution chemistry environments is recommended.

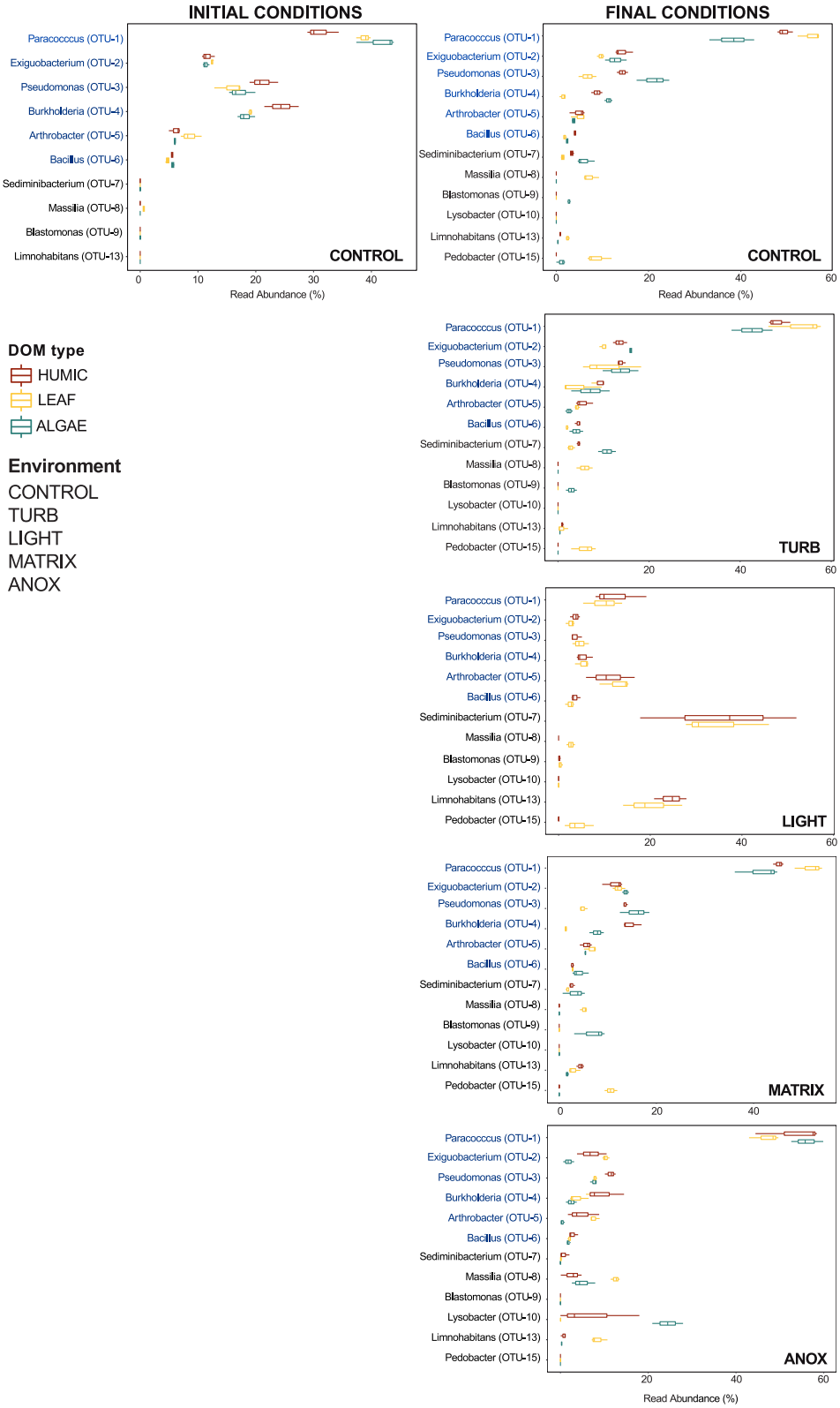

Fig 4. Relative abundance of the 12 prevalent OTUs under the different environments (panels: control, turbulence, UV-light, matrix, and anoxic) and DOM sources (colors: algae cultures [Algae], alder leaves leachates [Leaf], and Suwannee River Natural Organic Matter [Humic]). The relative OTU abundance has been corrected according to the rRNA operon copy number in the corresponding taxon and filtered by abundance (1% cutoff) (*see* "Material and methods" section for details). OTUs colored names in blue correspond to species in the SBI. Boxplots show median, hinges as to the first and third quartiles and whiskers correspond to the largest or smallest values at most 1.5 * IQR from the hinge (function *geom_boxplot* in ggplot2 package for R).

DOM fluorescent compositional changes during degradation are not systematic for a given environment, but a function of the DOM source

Previous studies have found a consistent degradation of specific organic compounds regardless of the DOM source (e.g., during biodegradation: D'Andrilli et al. 2019 or photodegradation experiments: Mostovaya et al. 2017). Thus, we expected a consistent effect of a given environmental condition on each fluorescence component across all DOM sources. However, results show that the relative change of fluorescence components was not consistent for a given environment, but dependent on the DOM source (Fig. 3). Indeed, while it is true that there was a generalized relative decrease in the protein-like fluorescence of component C1 and a relative accumulation of humic-like component C2, the magnitude of change was always a function of the DOM source. Conspicuous differential behavior across sources and environments was observed for the light treatment effect on the humic-like component C2 or for the strong relative decrease in component C3 for the leaf leachates' DOM across all the environments (Fig. 3b,c). This behavior, together with the constant pattern in relative change for component C1 across sources and the higher relevance of DOM_{source} over Environment, is evidence that the change in DOM composition was not uniform in each environment but highly dependent on the available constituents. Component C4 did not change significantly in most incubations, indicating that it might include persistent or tightly cycled DOM constituents.

To understand these results, it is fundamental to consider: first, that the analytical window of fluorescence spectroscopy is limited (Murphy et al. 2010) and second, that fluorescence components represent covarying families of molecular compounds (i.e., the constituents of C2 in algal DOM might not be the same as in C2 of leaf leachates' DOM) (Stubbins et al. 2014). Consequently, contrasting effects of the same environment across DOM sources might be expected. Component C1 consistently represented the main driver of bulk DOM degradation, as it decayed across DOM sources and environments and represents protein-like DOM, commonly interpreted as labile (Fellman et al. 2010). Component C2, attributed to aromatic, terrestrial, and most likely highly unsaturated compounds (Stubbins et al. 2014) is typically strongly affected by photo-decay (Stubbins et al. 2010). However, for C2, we only saw an effect of UV-light exposure ($Environment_{UV\ Light}$) in the humic DOM source. Similarly, component C3 was affected by degradation only in the case of leaf-litter-derived DOM, a source for which C3 accounted for most of the fluorescence (Supporting Information Fig. S1.1). Thus, the same component might be an indicator of different "families of compounds" in contrasting DOM sources, leading to divergent effects of the same environment across DOM sources, and highlighting that excitation-emission matrices components may not be strictly comparable across environments or between studies. The HPLC-ESI-HRMS results (Supporting Information Fig. S1.2) point toward a similar direction: very contrasted DOM sources had highly different solid phase extraction efficiencies, molecular formulas, chromatographic peak retention times, and broadness, indicating a large degree of chemical dissimilarity at the molecular level. Thus, conclusions from in situ studies assessing the effect of environment on contrasting organic matter sources based on molecular composition data and, especially when using solid-phase-extracted DOM, should be handled with care.

Environment prevails over DOM composition on shaping bacterial community composition

The functional versatility of the standard bacterial inoculum allowed us to properly test contrasting environments, including anoxic conditions. According to our results, the environment was the main driver of the changes observed in the composition of bacterial communities (Fig. 5). The effect of DOM source was also relevant but explained less variance along its corresponding axis, that showed a marked effect of incubation time. Overall, the standard bacterial inoculum community was dominant across all treatments, but the environment specifically contributed to enrich one species over the other depending on their metabolic capabilities and physiological requirements. This is not surprising based on general expected diversity patterns of microbial species in the environment (Fenchel and Finlay 2004). Nevertheless, it implies that the microbial function under study (i.e., DOM degradation) did not entirely depend on community composition, which is modeled by environmental factors, but rather on the organic substrate available.

It has been hypothesized that each of the individual compounds constituting DOM could be linked to a specific microbial degradation pathway (Osterholz et al. 2016). Although we did not aim to contribute to solve this conundrum, we designed an experimental approach not affected by differences in microbial composition (i.e., metabolic potential). By using the standard bacterial inoculum, we were able to remove this "microbial factor" from the equation, thus allowing us to discriminate between the effect of environmental conditions (i.e., the *soil*) and the DOM composition (i.e., the *seed*) on DOM degradation rates. In a previous study, we demonstrated that the standard bacterial inoculum was able to reproduce DOM biodegradation rates that are comparable to natural communities (Pastor et al. 2018), which is also the case in the current work (Table 1; Fig. 2). Moreover, except for the UV-light environment, the experimental design did not suffer from relevant bacterial contamination, as indicated by the prevalence of the standard bacterial inoculum strains at the end of the incubation time (Fig. 4). The dominant standard bacterial inoculum strain across treatments was the facultative anaerobe *Paracoccus denitrificans* (Pastor et al. 2018). In the case of the UV-light exposure environment, the bacterial community became enriched in sequences affiliated to *Sediminibacterium* genus (OTU-7, $\approx$ 40% of total reads), both in

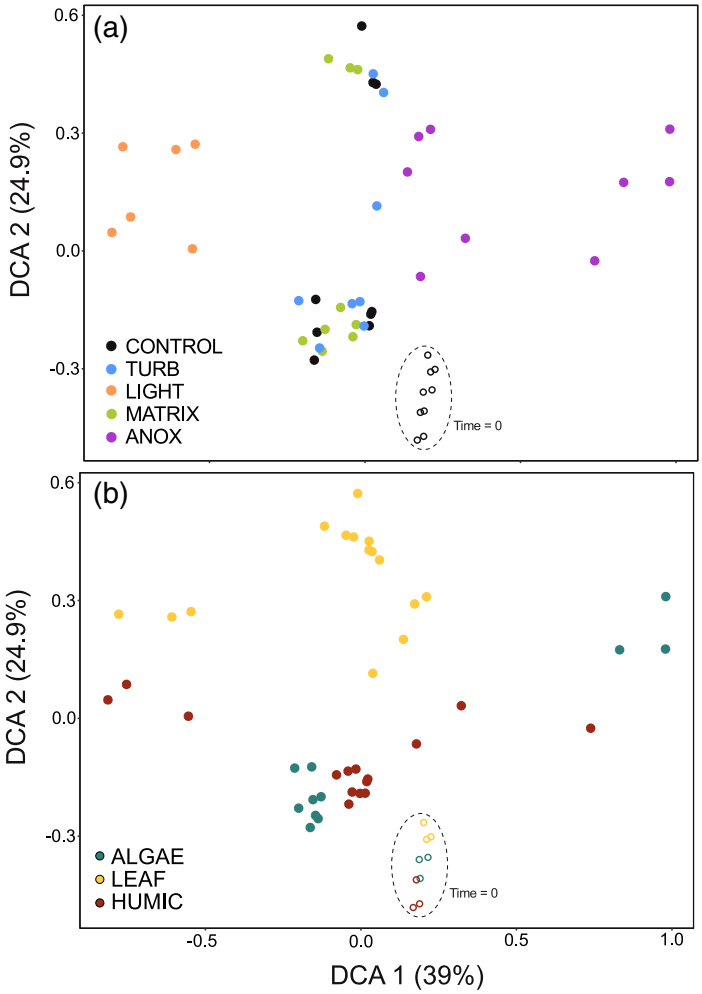

Fig 5. Detrended canonical analysis ordination based on Bray–Curtis similarity distance of bacterial communities developed in samples incubated under (**a**) different environments: control, turbulence, UV-light, matrix, and anoxic and (**b**) DOM sources: algae cultures (Algae), alder leaves leachates (Leaf), and Suwannee River Natural Organic Matter (Humic). Symbols corresponding to $t = 0$ of the incubation are empty and to t = final full.

the algal and leaf-litter-derived DOM sources (Fig. 4). We consider this contamination to have a minimal impact on the DOC degradation kinetics tested here. First, despite the high DOM decay under the light environment (Table 1), we do believe this corresponds to the effect of UV-light on DOM as reflected for fluorescent component C2 and discussed in the previous section. Second, the highest decay rates were measured for the leaf litter-derived DOM source without registering any relevant contamination in any other environment. Finally, the conspicuous contamination observed in the algal DOM under anoxic conditions (Fig. 4), did not correspond to an increase in DOM decay. Regarding the potential source of the observed contaminations, it is unlikely that *Sediminibacterium* was present in the standard bacterial inoculum at the beginning of the experiment considering the origin of the inoculum (pure cultures of the six reference strains) and the ecology of the contaminant microbe (members of the genus *Sediminibacterium* inhabit both natural [freshwater biofilms] and engineered environments [activate sludge digestors]; Qu and Yuan 2008; Singleton et al. 2011; Besemer et al. 2012). It is then more plausible to assume some contamination during preparation and handling of DOM sources. We thus strongly recommend testing axenic conditions using DNA analysis instead of microscopy identification as in previous studies addressing similar questions (Smith et al. 2018). In fact, natural DOM sources such as leaf litter or algal extracts likely contain indigenous bacteria that, under given environmental conditions, might develop and outcompete the reference strains during incubation time. This bacterial turnover might be hard to distinguish using the microscope, but easily detected using modern sequencing technologies (i.e., amplicon-based sequencing or metagenomics).

So far, neither the selective pressure of DOM structure on microbial community composition (Logue et al. 2016; Osterholz et al. 2016) nor the coupling between community composition and its function are well understood (Langenheder et al. 2005; Ruiz-González et al. 2015). According to our results, if these relationships are tested under different environments or DOM sources, we might easily fail to experimentally detect them. Although we do not aim to solve the molecules-pathways challenge posed above, our methodology and results provide relevant information on the biogeochemical functioning to face it. Thus, although the environment has the capacity to shape the bacterial community composition, the biogeochemical function exerted by this community still depended on the intrinsic nature of the DOM sources.

Conclusions

Our study indicates that DOM source is more important than environment in determining bulk DOC decay, although both have a significant effect for the conditions herein. Changes in DOM composition appear to be driven by the interaction between DOM source and environment, but it is important to take into account that the effects of narrow analytical windows restrict the comparison of the effect of a given environment on different DOM sources. Finally, the standard bacterial inoculum allows testing environment vs. composition controls on DOM decay and points toward the idea that the microbial community is affected by environment rather than by DOM source in the present study, without relevant consequences for the DOM degradation function.

References

Andersen, K. S., R. H. Kirkegaard, S. M. Karst, and M. Albertsen. 2018. ampvis2: An R package to analyse and visualise 16S rRNA amplicon data. bioRxiv 299537. doi:10.1101/299537

Argote, L., and J. M. Levine. 2020. The Oxford handbook of group and organizational learning. Oxford University Press. doi:10.1093/oxfordhb/9780190263362.001.0001

Besemer, K., H. Peter, J. B. Logue, S. Langenheder, E. S. Lindström, L. J. Tranvik, and T. J. Battin. 2012. Unraveling assembly of stream biofilm communities. ISME J. **6**: 1459–1468. doi:10.1038/ismej.2011.205

Caporaso, J. G., and others. 2010. QIIME allows analysis of high-throughput community sequencing data. Nat. Methods **7**: 335–336. doi:10.1038/nmeth..303

Chin, W. C., M. V. Orellana, and P. Verdugo. 1998. Spontaneous assembly of marine dissolved organic matter into polymer gels. Nature **391**: 568–572. doi:10.1038/35345

Cole, J. J., and others. 2007. Plumbing the Global Carbon Cycle: Integrating Inland Waters into the Terrestrial Carbon Budget. Ecosystems **10**: 172–185. doi:10.1007/s10021-006-9013-8

Creed, I. F., and others. 2015. The river as a chemostat: fresh perspectives on dissolved organic matter flowing down the river continuum. Canadian Journal of Fisheries and Aquatic Sciences **72**: 1272–1285. doi:10.1139/cjfas-2014-0400

D'Andrilli, J., J. R. Junker, H. J. Smith, E. A. Scholl, and C. M. Foreman. 2019. DOM composition alters ecosystem function during microbial processing of isolated sources. Biogeochemistry **142**: 281–298. doi:10.1007/s10533-018-00534-5

Dittmar, T. 2014. Reasons behind the long-term stability of dissolved organic matter, 2nf ed, 369–388. Biogeochemistry of Marine Dissolved Organic Matter. Elsevier. doi:10.1016/B978-0-12-405940-5.00007-8

Dittmar, T., B. Koch, N. Hertkorn, and G. Kattner. 2008. A simple and efficient method for the solid-phase extraction of dissolved organic matter (SPE-DOM) from seawater. Limnology and Oceanography: Methods **6**: 230–235. doi:10.4319/lom.2008.6.230

Fellman, J. B., E. Hood, and R. G. M. Spencer. 2010. Fluorescence spectroscopy opens new windows into dissolved organic matter dynamics in freshwater ecosystems: A review. Limnol. Oceanogr. **55**: 2452–2462. doi:10.4319/lo.2010.55.6.2452

Fenchel, T. O. M., and B. J. Finlay. 2004. The ubiquity of small species: Patterns of local and global diversity. Bioscience **54**: 777–784. doi:10.1641/0006-3568(2004)054[0777:TUOSSP]2.0.CO;2

Fox, J., and S. Weisberg. 2011. An R companion to applied regression, 2nd ed. Sage publisher.

Green, N. W., D. McInnis, N. Hertkorn, P. A. Maurice, and E. M. Perdue. 2015. Suwannee River natural organic matter: Isolation of the 2R101N reference sample by reverse osmosis. Environ. Eng. Sci. **32**: 38–44. doi:10.1089/ees.2014.0284

Hawkes, J. A., C. Patriarca, P. J. R. Sjöberg, L. J. Tranvik, and J. Bergquist. 2018. Extreme isomeric complexity of dissolved organic matter found across aquatic environments. Limnol. Oceanogr.: Lett. **3**: 21–30. doi:10.1002/lol2.10064

Hemingway, J. D., D. H. Rothman, K. E. Grant, S. Z. Rosengard, T. I. Eglinton, L. A. Derry, and V. V. Galy. 2019. Mineral protection regulates long-term global preservation of natural organic carbon. Nature **570**: 228–231. doi:10.1038/s41586-019-1280-6

Kellerman, A. M., D. N. Kothawala, T. Dittmar, and L. J. Tranvik. 2015. Persistence of dissolved organic matter in lakes related to its molecular characteristics. Nat. Geosci. **8**: 454–457. doi:10.1038/ngeo2440

Kleber, M. 2010. What is recalcitrant soil organic matter? Environ. Chem. **7**: 320–332. doi:10.1071/EN10006

Koch, B. P., K.-U. Ludwichowski, G. Kattner, T. Dittmar, and M. Witt. 2008. Advanced characterization of marine dissolved organic matter by combining reversed-phase liquid chromatography and T-ICR-MS. Mar. Chem. **111**: 233–241. doi:10.1016/j.marchem.2008.05.008

Koehler B., E. von Wachenfeldt, D. Kothawala, and L. J. Tranvik. 2012. Reactivity continuum of dissolved organic carbon decomposition in lake water. Journal of Geophysical Research: Biogeosciences **117**. doi:10.1029/2011jg001793

Kothawala, D. N., K. R. Murphy, C. A. Stedmon, G. A. Weyhenmeyer, and L. J. Tranvik. 2013. Inner filter correction of dissolved organic matter fluorescence. Limnol. Oceanogr.: Methods **11**: 616–630. doi:10.4319/lom.2013.11.616

Kujawinski E. B., M. A Freitas, X. Zang, P. G. Hatcher, K. B. Green-Church, and R. B. Jones. 2002. The application of electrospray ionization mass spectrometry (ESI MS) to the structural characterization of natural organic matter. Organic Geochemistry **33**: 171–180. doi:10.1016/s0146-6380(01)00149-8

Lakhotia, S. C. 2009. Nature of methods in science: Technology driven science versus science driven technology. Bioessays **31**: 1370–1371.

Langenheder, S., E. S. Lindström, and L. J. Tranvik. 2005. Weak coupling between community composition and functioning of aquatic bacteria. Limnol. Oceanogr. **50**: 957–967. doi:10.4319/lo.2005.50.3.0957

Lee Z. M.-P., C. Bussema, and T. M. Schmidt. 2009. rrnDB: documenting the number of rRNA and tRNA genes in bacteria and archaea. Nucleic Acids Research **37**: D489–D493. doi:10.1093/nar/gkn689

Llirós, M., E. O. Casamayor, and C. M. Borrego. 2008. High archaeal richness in the water column of a freshwater sulfurous karstic lake along an interannual study. FEMS Microbiol. Ecol. **66**: 331–342. doi:10.1111/j.1574-6941.2008.00583.x

Logue, J. B., C. A. Stedmon, A. M. Kellerman, N. J. Nielsen, A. F. Andersson, H. Laudon, E. S. Lindström, and E. S. Kritzberg. 2016. Experimental insights into the importance of aquatic bacterial community composition to the degradation of dissolved organic matter. ISME J. **10**: 533–545. doi:10.1038/ismej.2015.131

Mann P. J., and others. 2015. Utilization of ancient permafrost carbon in headwaters of Arctic fluvial networks. Nature Communications **6**. doi:10.1038/ncomms8856

Marín-Spiotta, E., K. E. Gruley, J. Crawford, E. E. Atkinson, J. R. Miesel, S. Greene, C. Cardona-Correa, and R. G. M. Spencer. 2014. Paradigm shifts in soil organic matter research affect interpretations of aquatic carbon cycling: Transcending disciplinary and ecosystem boundaries. Biogeochemistry **117**: 279–297. doi:10.1007/s10533-013-9949-7

McCallister S. L., and P. A. del Giorgio. 2012. Evidence for the respiration of ancient terrestrial organic C in northern temperate lakes and streams. Proceedings of the National Academy of Sciences **109**: 16963–16968. doi:10.1073/pnas.1207305109

McMurdie, P. J., and S. Holmes. 2013. phyloseq: An R package for reproducible interactive analysis and graphics of microbiome census data. PLoS One **8**: e61217. doi:10.1371/journal.pone.0061217

Moran, M. A., and others. 2016. Deciphering ocean carbon in a changing world. Proc. Natl. Acad. Sci. USA **113**: 3143–3151. doi:10.1073/pnas.1514645113

Mosher, J. J., L. A. Kaplan, D. C. Podgorski, A. M. McKenna, and A. G. Marshall. 2015. Longitudinal shifts in dissolved organic matter chemogeography and chemodiversity within headwater streams: A river continuum reprise. Biogeochemistry **124**: 371–385. doi:10.1007/s10533-015-0103-6

Mostovaya A., J. A. Hawkes, T. Dittmar, and L. J. Tranvik. 2017. Molecular Determinants of Dissolved Organic Matter Reactivity in Lake Water. Frontiers in Earth Science **5**. doi:10.3389/feart.2017.00106

Mukherjee, S. 2017. Cancer's invasion equation. *New Yorker*. https://www.newyorker.com/magazine/2017/09/11/cancers-invasion-equation

Murphy, K. R., K. D. Butler, R. G. M. Spencer, C. A. Stedmon, J. R. Boehme, and G. R. Aiken. 2010. Measurement of dissolved organic matter fluorescence in aquatic environments: An interlaboratory comparison. Environ. Sci. Technol. **44**: 9405–9412. doi:10.1021/es102362t

Murphy, K. R., C. A. Stedmon, D. Graeber, and R. Bro. 2013. Fluorescence spectroscopy and multi-way techniques. PARAFAC. Anal. Methods **5**: 6557–6566. doi:10.1039/c3ay41160e

Murphy, K. R., C. A. Stedmon, P. Wenig, and R. Bro. 2014. OpenFluor—an online spectral library of auto-fluorescence by organic compounds in the environment. Anal. Methods **6**: 658–661. doi:10.1039/C3AY41935E

Osterholz H., G. Singer, B. Wemheuer, R. Daniel, M. Simon, J. Niggemann, and T. Dittmar. 2016. Deciphering associations between dissolved organic molecules and bacterial communities in a pelagic marine system. The ISME Journal **10**: 1717–1730. doi:10.1038/ismej.2015.231

Pastor, A., N. Catalán, N. Nagar, T. Light, C. M. Borrego, and R. Marcé. 2018. A universal bacterial inoculum for dissolved organic carbon biodegradation experiments in freshwaters. Limnol. Oceanogr.: Methods **16**: 421–433. doi:10.1002/lom3.10256

Patriarca, C., J. Bergquist, P. J. R. Sjöberg, L. J. Tranvik, and J. A. Hawkes. 2018. Online HPLC-ESI-HRMS method for the analysis and comparison of different dissolved organic matter samples. Environ. Sci. Technol. **52**: 2091–2099. doi:10.1021/acs.est.7b04508

Pinheiro, J., D. Bates, S. DebRoy, D. Sarkar, and R Core Team. 2018. nlme: Linear and Nonlinear Mixed Effects Models. R package v. https://CRAN.R-project.org/package=nlme

Prairie, Y. T. 2008. Carbocentric limnology: Looking back, looking forward. Can. J. Fish. Aquat. Sci. **65**: 543–548. doi:10.1139/08-011

Qu, J. H., and H. L. Yuan. 2008. *Sediminibacterium salmoneum* gen. nov., sp. nov., a member of the phylum *Bacteroidetes* isolated from sediment of a eutrophic reservoir. Int. J. Syst. Evol. Microbiol. **58**: 2191–2194. doi:10.1099/ijs.0.65514-0

R Development Core Team, R (2016). A language and environment for Statistical Computing, Vienna. R Foundation for Statistical Computing.

Roger, F., S. Bertilsson, S. Langenheder, O. A. Osman, and L. Gamfeldt. 2016. Effects of multiple dimensions of bacterial diversity on functioning, stability and multifunctionality. Ecology **97**: 2716–2728. doi:10.1002/ecy.1518

Ruiz-González, C., J. P. Niño-García, J.-F. Lapierre, and P. A. del Giorgio. 2015. The quality of organic matter shapes the functional biogeography of bacterioplankton across boreal freshwater ecosystems. Glob. Ecol. Biogeogr. **24**: 1487–1498. doi:10.1111/geb.12356

Schmidt, M. W. I., and others. 2011. Persistence of soil organic matter as an ecosystem property. Nature **478**: 49–56. doi:10.1038/nature10386

Singleton, D. R., S. D. Richardson, and M. D. Aitken. 2011. Pyrosequence analysis of bacterial communities in aerobic bioreactors treating polycyclic aromatic hydrocarbon-contaminated soil. Biodegradation **22**: 1061–1073. doi:10.1007/s10532-011-9463-3

Sinsabaugh, R. L., and S. E. G. Findlay. 2003. Dissolved organic matter: Out of the black box into the mainstream, p. 479–496. *In*. S. E. G. Findlay and R. L. Sinsabaugh, (eds.). Aquatic ecosystems: Interactivity of dissolved organic matter. Elsevier Science.

Smith, H. J., M. Tigges, J. D. Andrilli, A. Parker, B. Bothner, and C. M. Foreman. 2018. Dynamic processing of DOM: Insight from exometabolomics, fluorescence spectroscopy, and mass spectrometry. Limnol. Oceanogr.: Lett. **3**: 225–235. doi:10.1002/lol2.10082

Sobek, S., L. J. Tranvik, Y. T. Prairie, P. Kortelainen, and J. J. Cole. 2007. Patterns and regulation of dissolved organic carbon: An analysis of 7,500 widely distributed lakes. Limnol. Oceanogr. **52**: 1208–1219. doi:10.4319/lo.2007.52.3.1208

Stubbins, A., and others. 2010. Illuminated darkness: Molecular signatures of Congo River dissolved organic matter and its photochemical alteration as revealed by ultrahigh

precision mass spectrometry. Limnol. Oceanogr. **55**: 1467–1477. doi:10.4319/lo.2010.55.4.1467

Stubbins A., J.-F. Lapierre, M. Berggren, Y. T. Prairie, T. Dittmar, and P. A. del Giorgio. 2014. What's in an EEM? Molecular Signatures Associated with Dissolved Organic Fluorescence in Boreal Canada. Environmental Science & Technology **48**: 10598–10606. doi:10.1021/es502086e

Subirats, J., A. Di Cesare, S. Varela della Giustina, A. Fiorentino, E. M. Eckert, S. Rodriguez-Mozaz, C. M. Borrego, and G. Corno. 2019. High-quality treated wastewater causes remarkable changes in natural microbial communities and *intI1* gene abundance. Water Res. **167**: 114895. doi:10.1016/j.watres.2019.114895

Wienhausen G., B. E. Noriega-Ortega, J. Niggemann, T. Dittmar, and M. Simon. 2017. The Exometabolome of Two Model Strains of the Roseobacter Group: A Marketplace of Microbial Metabolites. Frontiers in Microbiology **8**: doi:10.3389/fmicb.2017.01985

Acknowledgments

This study has been supported by the project C-HydroChange, funded by the Spanish Agencia Estatal de Investigación (AEI) and Fondo Europeo de Desarrollo Regional (FEDER) under the contract FEDER-MCIU-AEI/CGL2017-86788-C3-2-Pand CGL2017-86788-C3-3-P. Earlier steps of this research also benefited from the FREEDOM project, funded by the Spanish Ministry of Economy and Competitiveness (CGL2014–61771-EXP). NC held a Beatriu de Pinós postdoctoral grant (2016-00215) from the Catalan government and a Marie Sklodowska-Curie grant (agreement 839709) from the European Union's Horizon 2020 research and innovation program. DvS is a Serra Húnter Fellow. JPCR holds a Juan de la Cierva—Formación grant (FJC2018-037791-I) from the Spanish Ministry of Science and Innovation. ICRA researchers acknowledge the support for scientific equipment given by the European Regional Development Fund (FEDER) under the Catalan FEDER Operative Program 2007–2013 and by MINECO according to DA3ª of the Catalan Statute of Autonomy and to PGE-2010 as well as the funding from the CERCA program of the Catalan government. The authors thank Biel Obrador for his contribution on the initial design of the experiment and lab work. We thank Wolfgang Gernjak for the use of the radiometer and Miquel-Àngel Rodriguez-Arias for his support during the ideation workshop.

Conflict of Interest

None declared.

Submitted 27 November 2019
Revised 30 March 2020
Accepted 15 July 2020

Associate editor: Hans-Peter Grossart